Aalborg Universitet

AALBORG UNIVERSITY
DENMARK

Variable Speed Wind Turbine Based on Multiple Generators Drive-Train Configuration

Deng, Fujin; Chen, Zhe

Variable Speed Wind Turbine Based on Multiple Generators Drive-Train Configuration

Fujin Deng,   Zhe Chen,   *Senior Member, IEEE*

Abstract--A variable speed wind turbine is presented in this paper, where multiple permanent magnet synchronous generators (MPMSGs) drive-train configuration is employed in the wind turbine. A cascaded multilevel converter interface based on the MPMSGs is developed to synthesize a desired high ac sinusoidal output voltage, which could be directly connected to the grids. What is more, such arrangement has been made so that the output ac voltage having a selected phase angle difference among the stator windings of multiple generators. A phase angle shift strategy is proposed in this paper, which effectively reduce the fluctuation of the electromagnetic torque sum and results in a good performance for the MPMSGs structure. The simulation study is conducted using PSCAD/EMTDC, and the results verify the feasibility of this variable speed wind turbine based on multiple generators drive-train configuration.

Index Terms—Wind power generation, energy conversion, permanent magnet generators, variable speed wind turbine.

I. INTRODUCTION

A MONG the renewable energy technologies being vigorously developed, wind turbine technology has being undergoing a dramatic development and now is the world's fastest growing energy [1]. The future trend of wind energy conversion systems is to increase the power capacity of wind turbines and generators to reduce the cost of generated electricity. Currently, most installed wind turbine generators are in the power range of 1.5 to 5 MW. Numerous research efforts have been done for large systems, targeting 5-10 MW level for offshore applications [2].

The permanent magnet synchronous generator (PMSG), characterized as having large air gaps and reduces flux linkage even in machines with multi magnetic poles, has been proved to be an effective solution, especially for offshore applications, because of its low maintenance cost, wide operating range. Recently, a PMSG with a full-scale power converter configuration is becoming more attractive for wind turbines. The inserted full-scale power converter decoupled the generator and the grid, which results in that the disturbance in the grid has no direct effect on the generator. It effectively enhances the capability of fault ride through [3].

In this paper, a variable speed wind turbine shown in Fig. 1 is presented. The multiple-generator drive train configuration
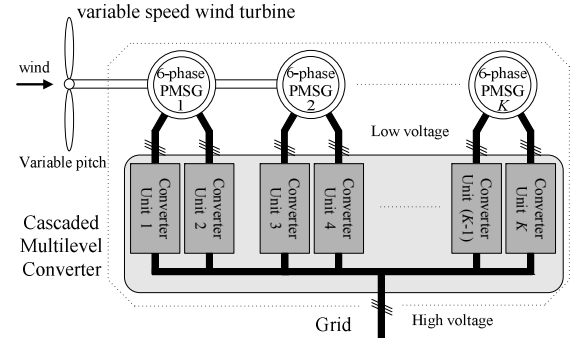

Fig. 1. Block diagram of a variable speed wind turbine based on multiple generators drive-train configuration and full-scale power converter.

is introduced these years, which appears to have significant cost reduction potential resulting from increased energy capture, simplified assembly, increased reliability, and reduced mass and so on [4]. A cascaded multilevel converter is applied between the generators and the grids. It could generate an almost sinusoidal and high ac three-phase voltage, which makes it possible for this structure wind turbine to be directly connected into the ac grids. A phase angle shift strategy of the generators' ac outputs is proposed for the multi-generator drive train configuration in this paper, which could effectively reduce the fluctuation of all the generators electromagnetic torque summation.

II. VARIABLE SPEED WIND TURBINE

The variable speed wind turbine, including the mechanical components, the electrical components and so on, is a complex electromechanical system. The model of the wind turbine is developed in the analysis tool PSCAD/EMTDC.

A. Aerodynamic Model

The mechanical power extracted from the wind can be expressed as follows [5],

$$P_w = \frac{1}{2}\rho\pi R^2 v^3 C_p(\theta,\lambda) \qquad (1)$$

where P_w is the extracted power from the wind, ρ is air density (kg/m^3), R is the blade radius (m), v is the wind speed(m/s) and C_P is the power coefficient which is a function of the pitch angle of rotor blades θ (deg) and of the tip speed ratio λ. The term λ is defined as $\lambda = \omega_w R/v$, with ω_w the wind turbine speed.

The power coefficient may be calculated as

Fujin Deng is with the Department of Energy Technology, Aalborg University, Aalborg, 9220, Denmark (e-mail: fde@iet.aau.dk).
Zhe Chen is with the Department of Energy Technology, Aalborg University, Aalborg, 9220, Denmark (e-mail: zch@iet.aau.dk).

$$C_p = 0.73(\frac{151}{\lambda_i} - 0.58\theta - 0.002\theta^{2.14} - 13.2) \cdot e^{-18.4/\lambda_i} \quad (2)$$

with

$$\frac{1}{\lambda_i} = \frac{1}{(\lambda - 0.02\theta)} - \frac{0.003}{(\theta^3 + 1)} \quad (3)$$

The wind turbine power coefficient is maximized C_{p_max}=0.44 for the optimal tip-speed ratio value λ_{opt} = 6.9 when the blades pitch angle is $\theta = 0^o$.

For each wind speed, there exists a specific point in the wind turbine output power versus rotating-speed characteristic where the output power is maximized. The control of the wind turbine results in a variable-speed wind turbine operation, such that maximum power is extracted continuously from the wind below the rated wind speed. Besides, the wind turbine operates at the rated power during the period of high wind speed by the variable-pitch regulation [6]-[8].

Based on (1) ~ (3), the relation between the optimal power and the wind turbine speed below the rated wind speed can be obtained below.

$$P_{w\_max} = \frac{1}{2}\rho\pi R^5 \frac{C_{p\_max}}{\lambda_{opt}^3} \cdot \omega_w^3 \quad (4)$$

Combing the wind turbine characteristic in Appendix and the maximum power point tracking (MPPT) method [9], the rotor speed versus power characteristic that leads to optimal energy capture is developed as Fig. 2. In order to avoid large power fluctuations when rotor speed changes near the minimum and nominal rotor speed, a control characteristic similar to that leads to optimal energy capture are adopted [10]. The control characteristic is depicted by the curves AB and CD in Fig. 2.

B. Mechanical Drive Train

In this paper, these PMSGs are installed on a common shaft. According to [11], a comparative study of wind turbine generator system using different drive train models, it has been shown that the two-mass model is suitable for transient stability analysis. Owing to the bigger mass of wind turbine than that of generator, Fig. 3 shows the simplified drive train for this wind turbine configuration. Referring to [8] and [11], the drive train mode shown in Fig. 3 could be obtained below.
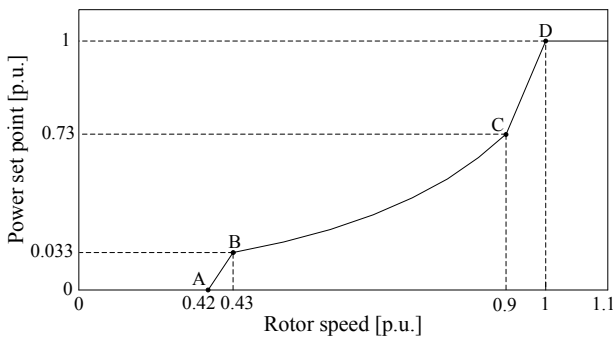

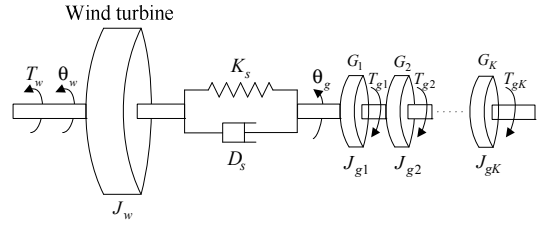Fig. 2. Optimal rotor speed versus power characteristic.

Fig. 3. Block diagram of the drive train model.

$$\begin{cases} J_w \frac{d\omega_w}{dt} = T_w - D_s(\omega_w - \omega_g) - K_s\theta_{wg} \\ \sum_K^{i=1} J_{gi} \frac{d\omega_g}{dt} = D_s(\omega_w - \omega_g) + K_s\theta_{wg} - \sum_K^{i=1} T_{gi} \end{cases} \quad (5)$$

where J_w and J_g are the equivalent wind turbine inertia and generator inertia respectively. Torque T_w and T_g represent the aerodynamic torque of the wind turbine and the generator loading torque, respectively. ω_w and ω_g are the wind turbine and generator rotor speed respectively. θ_{wg} is the angle between the turbine rotor and the generator rotor. K_s is the elastic characteristic of the shaft. D_s is the mutual damping. K is the number of generators.

C. Wind Turbine Model

A variable speed wind turbine including multiple-generator drive train configuration shown in Fig. 4 is presented here, where a few six-phase PMSGs are placed in one nacelle and driven by the same wind turbine in one shaft. The cascaded multilevel converter is used to control these PMSGs to capture the optimal energy from the wind, and step the low ac output voltage of the generators to a high ac level.

In Fig. 4, the six-phase PMSG is modeled referring to [12], which could effectively cancel out some dominant harmonics produced by the diode rectifiers [13], [14]. In this paper, the three-phase windings of PMSG are separated with each other without connection, which is used to isolate the electrical interface among converter modules in the cascaded converter shown in Fig. 5. The power output of the generator is restricted by the inductance of the coils. Herein, a capacitor is connected in parallel with the coil so as to cancel part of the inductance [15]. In each converter module, the ac output from the generator is converted to dc through diode rectifier. The boost converter is adopted here with a constant switching
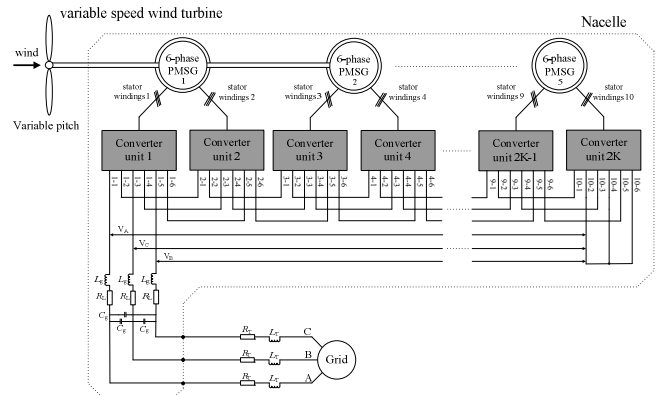

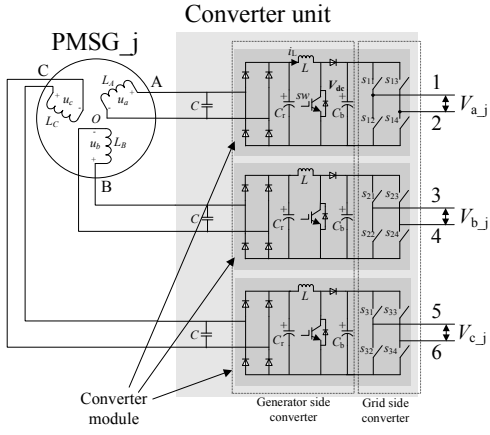Fig. 4. Block diagram of the variable speed wind turbine.

Fig. 5. Circuit configuration of single PMSG with a detailed, three-phase windings converter unit.

frequency as 1 kHz to stabilize the dc-links as 1.1 kV. The single-phase H-bridge converter referring to [16] is applied here with 1 kHz switching frequency to produce single-phase sinusoidal voltage.

The electrical configuration of five PMSGs is depicted by Fig. 4, where a particular phase of each set of three-phase stator windings is connected to the same phase of the other sets of stator windings through the converter modules which are connected in series at the output sides. A phase-shifted unipolar sinusoidal PWM (SPWM) switching scheme referring to [17] is used for the cascaded multi-level converter to synthesize a high ac voltage. Since each series connected H-bridge converter unit is electrically isolated, the total output voltage is the sum of each H-bridge outputs in the multilevel converter configuration. Hence, it is possible for the wind turbine with this structure to be directly connected into ac grids.

III. PROPOSED PHASE ANGLE SHIFT STRATEGY

The use of the diode rectifier to convert the generator output ac power to dc results in the pulsation appears in the stator current and the developed torque [15], [18], since the diode rectifier produces harmonic components in the stator current.

In this paper, these PMSGs are installed on a common shaft, where the output ac voltage of the stator windings among these generators has a selected phase angle shift. A schematic representation of the phase angle shift arrangements in a two-PMSG structure is shown in Fig. 6. Owing to the symmetry, the stator winding current fundamental components in i^{th} PMSG can be written below.

$$\begin{cases} i_{ai}(t) = I_m \cos(\omega_r t + \varphi + \theta_i) \\ i_{bi}(t) = I_m \cos(\omega_r t + \varphi + \theta_i - 2\pi/3) \\ i_{ci}(t) = I_m \cos(\omega_r t + \varphi + \theta_i + 2\pi/3) \end{cases} \quad (6)$$

$$\begin{cases} i_{xi}(t) = I_m \cos(\omega_r t + \varphi + \theta_i + \pi/6) \\ i_{yi}(t) = I_m \cos(\omega_r t + \varphi + \theta_i + \pi/6 - 2\pi/3) \\ i_{zi}(t) = I_m \cos(\omega_r t + \varphi + \theta_i + \pi/6 + 2\pi/3) \end{cases} \quad (7)$$
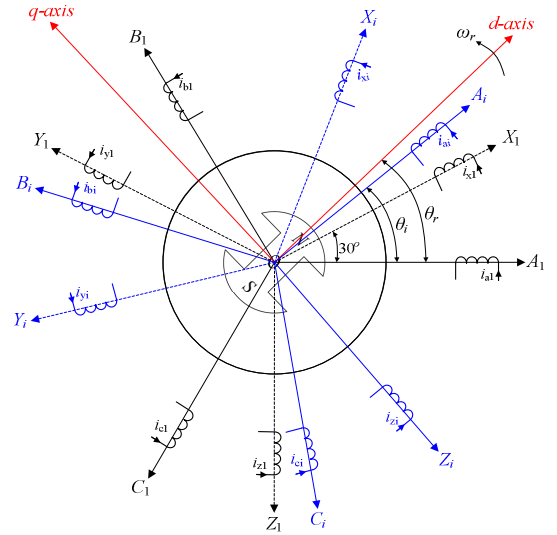

Fig. 6. Physical arrangement of the stator windings phase angle shift for 1st and i^{th} PMSGs in multiple generators structure.

where ω_r is the generator rotor speed, φ is the arbitrary phase angle, θ_i is the phase shift angle between the two PMSGs stator windings as shown in Fig. 6.

The influence to the electromagnetic torque sum coming from some harmonic components in stator current is analyzed in this section, where the positive-sequence, negative-sequence and zero-sequence components are considered respectively.

A. Positive-Sequence and Zero-Sequence Components

The physical arrangement of the stator windings is shown in Fig. 6. Owing to the symmetry, one of the stator windings current positive-sequence harmonic components in i^{th} PMSG could be expressed as follows.

$$\begin{cases} i_{afi}(t) = I_{mf} \cos(\omega_f t + \alpha + \theta_i) \\ i_{bfi}(t) = I_{mf} \cos(\omega_f t + \alpha + \theta_i - 2\pi/3) \\ i_{cfi}(t) = I_{mf} \cos(\omega_f t + \alpha + \theta_i + 2\pi/3) \end{cases} \quad (8)$$

$$\begin{cases} i_{xfi}(t) = I_{mf} \cos(\omega_f t + \alpha + \theta_i + \pi/6) \\ i_{yfi}(t) = I_{mf} \cos(\omega_f t + \alpha + \theta_i + \pi/6 - 2\pi/3) \\ i_{zfi}(t) = I_{mf} \cos(\omega_f t + \alpha + \theta_i + \pi/6 + 2\pi/3) \end{cases} \quad (9)$$

where α is the arbitrary phase angle, ω_f is this harmonic component angle speed. The other positive-sequence harmonic components could be analyzed with the same method, and with the similar results, which are not detailed analyzed here.

Considering the fundamental components and the positive-sequence harmonic component, using the transformation function in Appendix, the electromagnetic torque for the i^{st} PMSG could be obtained as follows.

$$T_{e\_i}^p(t) = T_{e\_i}^{p\_\omega r}(t) + T_{e\_i}^{p\_\omega f}(t) \quad (10)$$

with

$$T_{e\_i}^{p\_\omega r}(t) = -3n_p(L_{md} - L_{mq})I_m^2 \cdot \sin 2\varphi - 3n_p\psi_f I_m \cdot \sin\varphi$$

$$T_{e\_i}^{p\_\omega f}(t) = [6n_p(L_{md} - L_{mq})I_m I_{mf} \cdot \cos\varphi + 3n_p\psi_f I_{mf}]$$

$$\cdot \sin[(\omega_r - \omega_f)t - \alpha] - 6n_p(L_{md} - L_{mq})I_m I_{mf} \cdot \sin\varphi$$

$$\cdot \cos[(\omega_r - \omega_f)t - \alpha] + 3n_p(L_{md} - L_{mq})I_{mf}^2 \cdot \sin[2(\omega_r - \omega_f)t - 2\alpha]$$

The ith PMSG electromagnetic torque is composed with two parts, including $T_{e\_i}^{p}{}^{\omega r}(t)$ the fundamental electromagnetic torque component; $T_{e\_i}^{p}{}^{\omega f}(t)$ the pulsation torque resulted from the positive-sequence harmonic component in the stator windings current.

It is obvious that the angle θ_i shift in the ith PMSG would not cause some change to its electromagnetic torque produced by the positive-sequence harmonic components in the stator current.

Consequently, the electromagnetic torque summation of K PMSGs could be obtained below.

$$T_{e\_sum}^{p}(t) = \sum_{j=1}^{K} T_{e\_j}^{p}(t) = K \cdot T_{e\_1}^{p}(t) \tag{11}$$

It can be seen that the $T_{e\_sum}^{p}(t)$ in the multiple PMSGs structure could not be affected by the regulation of angle θ_i shift under the condition only with fundamental and positive-sequence harmonic components in the stator current.

With the same analysis method, the result only considering fundamental and zero-sequence harmonic components is the same to that with the fundamental and positive-sequence components, which is not detailed described here.

B. Negative-Sequence Components

The combination of fundamental and negative-sequence components is considered here. According to the symmetry, one of the stator winding current negative-sequence harmonic components in i^{th} PMSG could be expressed as (12) and (13). The other negative-sequence harmonic components could be analyzed with the same method, which are not depicted here.

$$\begin{cases} i_{afi}(t) = I_{mf}\cos(\omega_f t + \alpha + \theta_i) \\ i_{bfi}(t) = I_{mf}\cos(\omega_f t + \alpha + \theta_i + 2\pi/3) \\ i_{cfi}(t) = I_{mf}\cos(\omega_f t + \alpha + \theta_i - 2\pi/3) \end{cases} \tag{12}$$

$$\begin{cases} i_{xfi}(t) = I_{mf}\cos(\omega_f t + \alpha + \theta_i + \pi/6) \\ i_{yfi}(t) = I_{mf}\cos(\omega_f t + \alpha + \theta_i + \pi/6 + 2\pi/3) \\ i_{zfi}(t) = I_{mf}\cos(\omega_f t + \alpha + \theta_i + \pi/6 - 2\pi/3) \end{cases} \tag{13}$$

Using the transformation function in Appendix, combing (6)~(7) and (12)~(13), the electromagnetic torque for the i^{st} PMSG could be obtained as follows.

$$T_{e\_i}^{n}(t) = T_{e\_i}^{n}{}^{\omega r}(t) + T_{e\_i}^{n}{}^{\omega f}(t) \tag{14}$$

with

$$T_{e\_i}^{n}{}^{\omega r}(t) = -3n_p(L_{md} - L_{mq})I_m^2 \cdot \sin 2\varphi - 3n_p\psi_f I_m \cdot \sin\varphi$$

$$T_{e\_i}^{n}{}^{\omega f}(t) = [6n_p(L_{md} - L_{mq})I_m I_{mf} \cdot \cos\varphi + 3n_p\psi_f I_{mf}] \cdot \cos(\pi/6)$$

$$\cdot \sin[(\omega_r + \omega_f)t + \alpha + \pi/6 + 2\theta_i] - 6n_p(L_{md} - L_{mq})I_m I_{mf} \cdot \sin\varphi$$

$$\cdot \cos(\pi/6) \cdot \cos[(\omega_r + \omega_f)t + \alpha + \pi/6 + 2\theta_i] + \frac{9}{4}n_p(L_{md} - L_{mq})I_{mf}^2$$

$$\cdot \sin[2(\omega_r + \omega_f)t + 2\alpha + \pi/3 + 4\theta_i]$$

The $T_{e\_i}^{n}{}^{\omega r}(t)$ is the fundamental electromagnetic torque component. The $T_{e\_i}^{n}{}^{\omega f}(t)$ is the pulsation torque resulted from the negative-sequence harmonic component in the stator windings current, which is the function of the shift angle θ_i.

As to the K numbers of six-phase PMSGs, the summation of the electromagnetic torque pulsations could be easily obtained below.

$$T_{e\_pul}^{n}(t) = \sum_{K}^{i=1} T_{e\_i}^{n}(t) \tag{15}$$

$$= [6n_p(L_{md} - L_{mq})I_m I_{mf} \cdot \cos\varphi + 3n_p\psi_f I_{mf}] \cdot \cos(\pi/6)$$

$$\cdot \sum_{K}^{i=1} \sin[(\omega_r + \omega_f)t + \alpha + \pi/6 + 2\theta_i] - 6n_p(L_{md} - L_{mq})$$

$$\cdot I_m I_{mf}\sin\varphi\cos(\pi/6)\sum_{K}^{i=1}\cos[(\omega_r + \omega_f)t + \alpha + \pi/6 + 2\theta_i]$$

$$+ \frac{9}{4}n_p(L_{md} - L_{mq})I_{mf}^2 \sum_{K}^{i=1}\sin[2(\omega_r + \omega_f)t + 2\alpha + \pi/3 + 4\theta_i]$$

The torque pulsation component is composed with two kinds of harmonic variations. One is with the frequency $(\omega_r + \omega_f)$, and the other one is in the frequency $2(\omega_r + \omega_f)$. From (15), it is easy to see that the torque pulsation $T_{e\_pul}^{n}(t)$ during the negative-sequence current component could be canceled with the following two conditions.

(1) K is odd umber;

(2) $\theta = \delta \cdot \dfrac{\pi}{K}$.　　　　　($\delta$ is integer but not 0)

where θ is the angle between the neighbor two generators. Hence, in order to reduce the electromagnetic torque pulsation in the multiple generators structure with K numbers of PMSGs, the shift angle θ_i for the ith PMSG could be set as follows.

$$\theta_i = \delta \cdot \frac{\pi}{K} \cdot (i-1) \tag{16}$$

IV. SYSTEM SIMULATION

A 5 MW variable speed wind generation system is modeled as Fig. 4, which is composed with five 1 MW six-phase PMSGs to meet the condition (1) in section III. Major system parameters are listed in Appendix. In Fig. 4, 10 converter modules with the same phase are connected in series with each other to make up one 21-level cascaded multilevel converter. There are three cascaded multilevel converters in the wind turbine to construct three phases to be directly interfaced with the ac grid with the line-to-line voltage as 11 kV. It means a nominal current peak of 371 A for 5 MW power deliver. In this simulation, the transmission cable with a cross section area of 400 mm^2 is applied for the 5 km power delivery, where the resistance and the inductance of this cable are approximately 0.047 Ω/km and 0.00035 H/km respectively. The wind model is the standard component model from the PSCAD library referring to [18].

A. Simulation of Variable Speed Wind Turbine

In order to evaluate the dynamic performance of the wind turbine to capture the optimal energy and limit the pulsation of the electromagnetic torque summation, a variable wind speed is adopted here. According to the condition (2), the shift angle θ for the 5 PMSGs is set as 36° (δ=1).

Fig. 7(a) shows a variable wind speed in average as rated value. Here, the wind turbine speed is almost around the rated value and limited by the action of variable-pitch control system. Fig. 7(c) shows the summation of generator electromagnetic torque, which regulates the wind turbine speed to capture the optimal wind energy.

The dc-link voltage V_{dc} in the 1st PMSG system is given in Fig. 7 (d), which is kept constant as 1.1 kV by the corresponding boost converters. The other dc-link voltage in the other four PMSGs system is stabilized as 1.1 kV too. Fig. 7(e) gives 6 isolated stator windings power in the 1st PMSG, which is almost the same with each other. The other isolated stator windings power in the other PMSGs is almost similar to Fig. 7(e). In addition, the 5 PMSGs power are shown in Fig. 7(f) as well. It is easy to recognize that the five PMSGs equalize the power share captured from the wind. The active power and the reactive power sent to the grid by this wind turbine are shown in Fig. 7(g), which shows its optimal power tracking performance. The reactive power is regulated as 0 here. Finally, the windings 1 voltage u_{abc} and current i_{abc} in 1st PMSG is given in Fig. 7(h) and (i). Both of them are nearly symmetrical three-phase voltage and current.
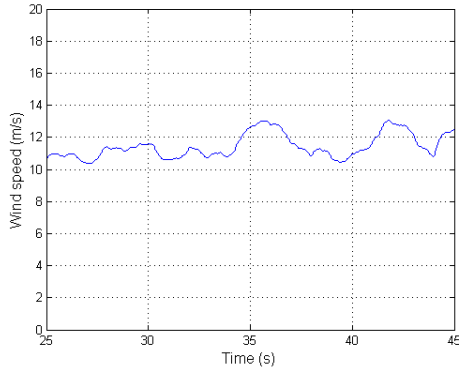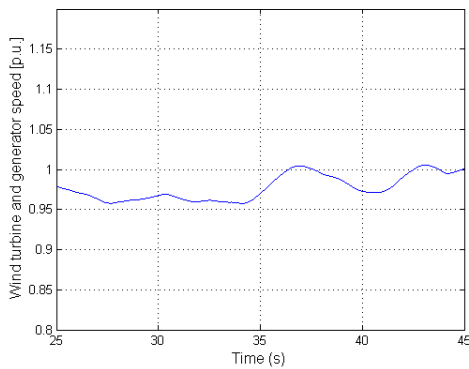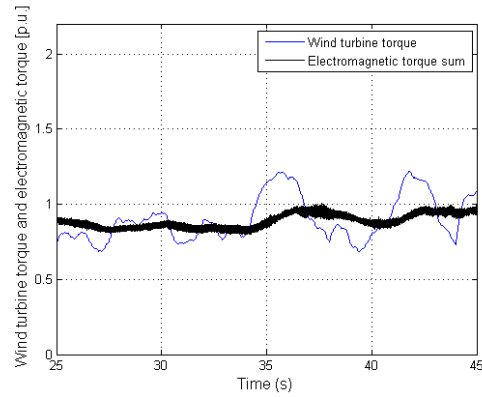

Fig. 7(c). Wind turbine torque and electromagnetic torque sum.
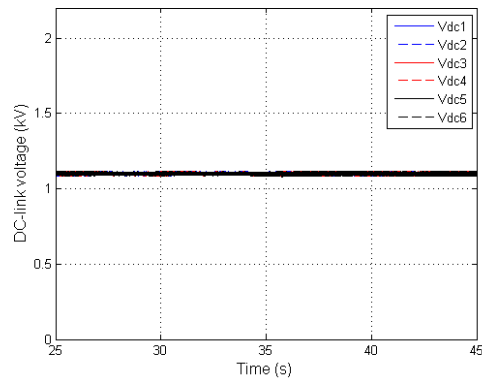
Fig. 7(d). DC-link voltage.

Fig. 7(a). Wind speed.

Fig. 7(e). Stator windings power in the 1st PMSG.

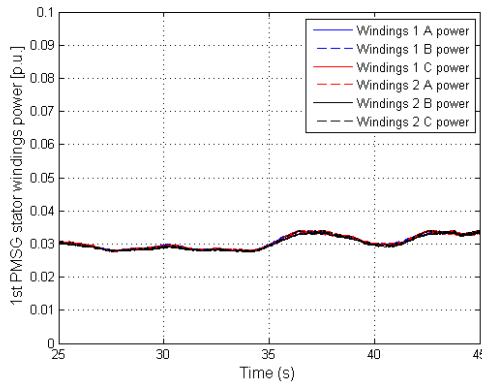
Fig. 7(b). Wind turbine speed.
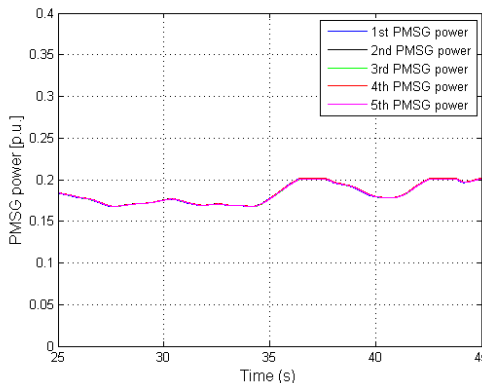

Fig. 7(f). PMSGs power in the wind turbine.
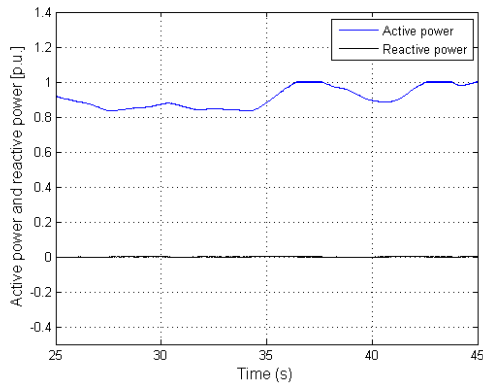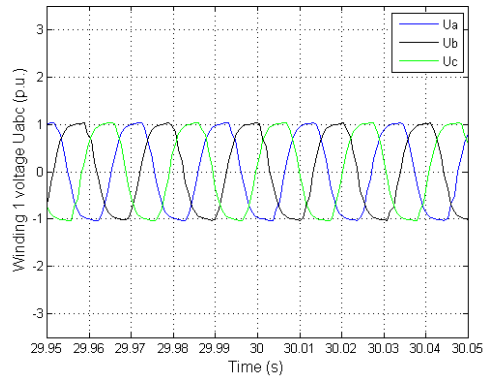
Fig. 7(g). Wind turbine active power and reactive power.

Fig. 8 (b). PMSG electromagnetic torque under 36° shift.

Fig. 7(h). The 1st PMSG stator windings voltage u_{abc}.

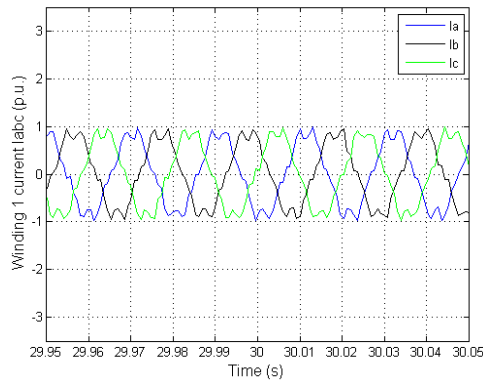Fig. 8(c). PMSG electromagnetic torque under 72° shift.

Fig. 7(i). The 1st PMSG stator windings current i_{abc}.
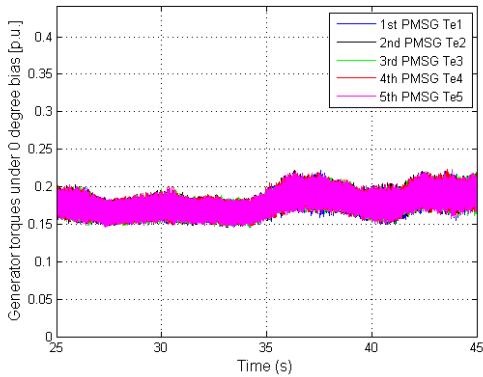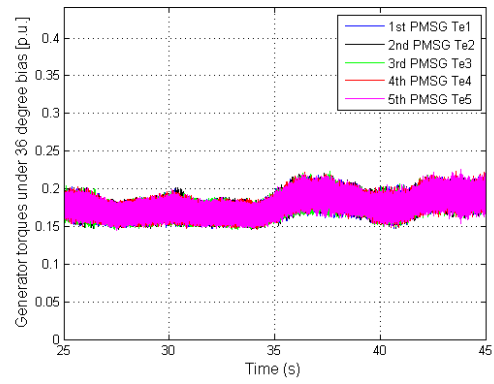

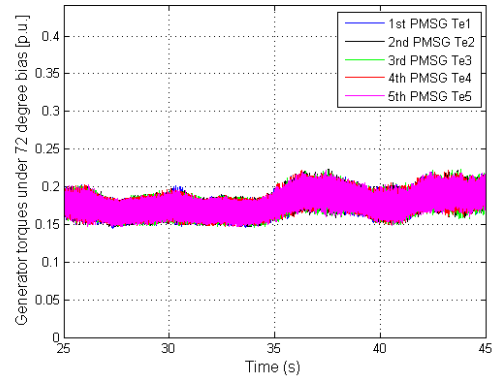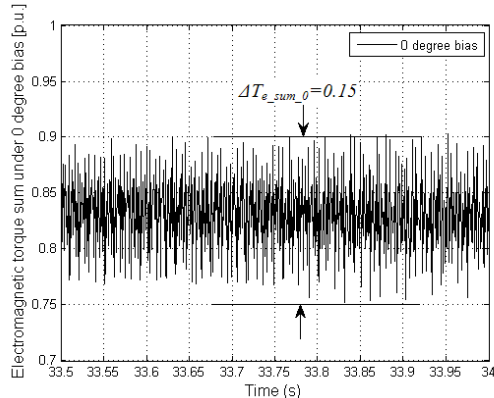Fig. 8(d). Electromagnetic torque sum under 0° shift.

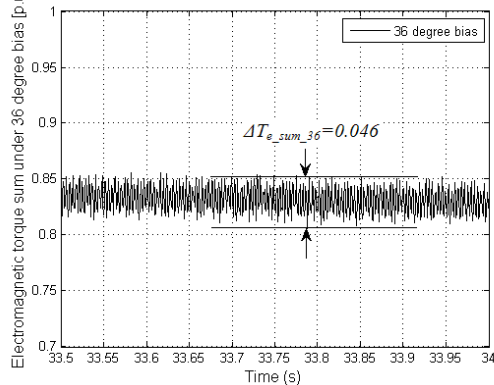Fig. 8(a). PMSG electromagnetic torque under 0° shift.

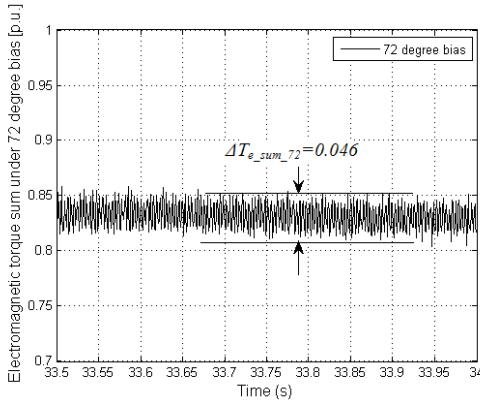Fig. 8(e). Electromagnetic torque sum under 36° shift.

Fig. 8(f). Electromagnetic torque sum under 72° shift.

B. Comparison of Electromagnetic Torque Pulsation

In this section, the proposed phase angle shift strategy is evaluated. The pulsation situations of the electromagnetic torque summation under three different shift angles θ including 0°, 36°, 72°, are simulated and contrasted in Fig. 8. Fig. 8(a)~(c) demonstrate the individual electromagnetic torque of the five PMSGs under the different angle shift. It indicates that the individual electromagnetic torque of the different PMSGs is almost the same to each other. However, the shift angle causes the change of the summation of the electromagnetic torques. It is easy to see that the 0° shift angle produces a biggest pulsation as 0.15 per unit among them. Fig. 8(e) and (f) show the improvement brought about by the proposed phase angle shift strategy. The 36° and 72° shift angles generate the same torque pulsation only as 0.046 per unit, which is only 30% of that in 0° shift. It is obvious to see that the proposed phase angle shift strategy makes a perfect performance for this wind turbine structure.

V. Conclusion

A variable speed wind turbine is presented, where the multiple generators drive train configuration is adopted. A few PMSGs are placed in one nacelle and driven by the same wind turbine, which effectively increases the wind turbine capacity and enhances the reliability. The cascaded multilevel converter technology is applied in the wind turbine, which could step up the output ac voltage of generator to a high level. Hence, the wind turbine could be directly integrated into the ac grids. A phase angle shift strategy for the multiple generators drive train configuration is proposed, where the output ac voltage having a suitable phase angle difference among the stator windings of multiple generators. This arrangement could effectively reduce the pulsation of the generator electromagnetic torque summation.

VI. Appendix

TABLE I
WIND TURBINE AND GENERATOR CHARACTERISTIC

Wind turbine rated power (MW)	5
Rotor diameter (m)	120
Rotating speed (r/m)	5.5~12.8
Nominal wind speed (m/s)	11.8
Generator Rated power (MW)	1
Phases	6
Stator rated line voltage (V)	690
Rated frequency (Hz)	50
Number of pole pairs	233
Stator winding resistance (p.u.)	0.0005
Windings 1 leakage reactance X_{l1} (p.u.)	0.012
Windings 2 leakage reactance X_{l2} (p.u.)	0.012
Inter-phase mutual reactance X_{md} (p.u.)	0.08
Inter-phase mutual reactance X_{mq} (p.u.)	0.08
stator windings mutual leakage X_{lqd} (p.u.)	0
Magnetic strength (p.u.)	1.2
Generator inertia (s)	0.5
Equivalent wind turbine inertia (s)	12.5
Shaft stiffness Ks (p.u.)	0.4
Shaft damping Ds (p.u.)	0.01

TABLE II
CASCADED MULTILEVEL CONVERTER CHARACTERISTIC

Capacitor C_r (F)	0.035
Induction L (H)	0.001
Capacitor C_b (F)	0.035
Resistance R_f (Ω)	0.00157
Induction L_f (H)	0.0005

ABC TO DQ0 TRANSFORMATION FUNCTION

$$\begin{bmatrix} U_d \\ U_q \\ U_0 \end{bmatrix} = \frac{2}{3} \begin{bmatrix} \cos\theta & \cos(\theta - 2\pi/3) & \cos(\theta + 2\pi/3) \\ \sin\theta & \sin(\theta - 2\pi/3) & \sin(\theta + 2\pi/3) \\ 1/2 & 1/2 & 1/2 \end{bmatrix} \cdot \begin{bmatrix} U_a \\ U_b \\ U_c \end{bmatrix}$$

DQ0 TO ABC TRANSFORMATION FUNCTION

$$\begin{bmatrix} U_a \\ U_b \\ U_c \end{bmatrix} = \begin{bmatrix} \cos\theta & \sin\theta & 1 \\ \cos(\theta - 2\pi/3) & \sin(\theta - 2\pi/3) & 1 \\ \cos(\theta + 2\pi/3) & \sin(\theta + 2\pi/3) & 1 \end{bmatrix} \cdot \begin{bmatrix} U_d \\ U_q \\ U_0 \end{bmatrix}$$

VII. Reference

[1] Z. Chen, Y. Hu, F. Blaabjerg, "Stability improvement of induction generator-based wind turbine systems," *Renewable Power Generation, IET*, vol. 1, pp. 81-93, March 2007.

[2] Jingya Dai, D. D. Xu, Bin Wu, "A novel control scheme for current-source-converter-based PMSG wind energy conversion systems," *IEEE Transactions on Power Electronics*, vol. 24, No. 4, pp. 963-972, April 2009.

[3] Zhe Chen, J. M. Guerrero, F. Blaabjerg, "A review of the state of the art of power electronics for wind turbines," *IEEE Transactions on Power Electronics*, vol. 24, Issue 8, pp. 1859-1875, August 2009.

[4] J. Cotrell, "A preliminary evaluation of a multiple-generator drivetrain configuration for wind turbines," *21th American Society of Mechanical Engineers (ASME) Wind Energy Symposium*, Jan. 2002.

[5] Tao Sun, Zhe Chen, Frede Blaabjerg, "Transient Stability of DFIG Wind Turbines at an External Short-Circuit Fault," *Wind Energy*. vol. 8, pp.345-360, August 2005.

[6] Tao Sun, Zhe Chen, F. Blaabjerg, "Flicker Study on Variable Speed Wind Turbines with Doubly Fed Induction Generators", *IEEE Transactions on Energy Conversion*, vol. 20, Issue 4, pp.896 – 905, December 2005.

[7] E. Muljadi, C. P. Butter field, "Pitch-controlled variable-speed wind turbine generation," *Industry Applications, IEEE Transaction*, vol. 37, pp. 240-246, Jan/Feb 2001.

[8] Fujin Deng, Zhe Chen, "Power control of permanent magnet generator based variable speed wind turbines," *ICEMS 2009*, pp. 1-6.

[9] V. Valtchev, A. Bossche, J. Ghijselen, J. Melkebeek, "Autonomous renewable energy conversion system," *Renew. Energy*, vol. 19, no. 1, pp.259-275, Jan. 2000.

[10] J. G. Slootweg, S.W.H. de Haan, H. Polinder, W.L. Kling, "General model for representing variable speed wind turbines in power system dynamics simulations," *IEEE Trans. Power System*, vol. 18, pp. 144–151, February 2003.

[11] S. M. Muyeen, Md. Hasan, R. Takahashi, T. Murata, J. Tamura, Y. Tomaki, A. Sakahara, E. Sasano, "Comparative study on transient stability analysis of wind turbine generator system using different drive train models," *IET Renew. Power Gener.*, 2007, 1, (2), pp. 131-141.

[12] Chee-Mun Ong, *Dynamic Simulation of Electric Machinery Using Matlab/Simulink*. New Jersey: Prentice Hall PTR, 1998, Chap. 7.

[13] R. F. Schiferl, C. M. Ong, "Six Phase synchronous Machine with AC and DC Stator Connections, Part II: Harmonic Studies and a Proposed Uninterruptible Power Supply Scheme", *IEEE Transactions on Power Apparatus and Systems*, vol. PAS-102, Issue 8, pp: 2694-2701, August 1983.

[14] Zitao Wang, Liuchen Chang, "A hybrid control method for six-phase permanent synchronous machine," *Electrical and Computer Engineering, CCECE 2008. Canadian Conference*, May 2008, pp. 575-578.

[15] Z. Chen, E. Spooner, W. T. Norris, A. C. Williamson, "Capacitor-Assisted Excitation of Permanent-Magnet Generators", *IEE Proc. Electric Power Applications*, vol. 145, Issue 6, pp. 497-508, November 1998.

[16] F. Blaabjerg, Zhe Chen, S. B. Kjaer, "Power electronics as efficient interface in dispersed power generation systems," *IEEE Transaction on Power Electronics*, vol. 19, Issue 5, pp.1184-1194, September 2004.

[17] Park Young-Min, Yoo Ji-Yoon, Lee Sang-Bin, "Practical implementation of PWM synchronization and phase-shift method for cascaded H-bridge multilevel inverters based on a standard serial communication protocol," *IEEE Transactions on Industry Applications*, vol. 44, No. 2, pp. 634-643, March/April 2008.

[18] Li Wang, Shiang-Shong Chen, Wei-Jen Lee, Zhe Chen, "Dynamic Stability Enhancement and Power Flow Control of a Hybrid Wind and Marine-Current Farm Using SMES," *IEEE Transactions on Energy Conversion*, vol. 24, Issue 3, pp. 626-639, September 2009.

VIII. Biographies

Fujin Deng received the B.Eng. degree in electrical engineering from China University of Mining and Technology, Jiangsu, China, in 2005. He received the M. Sc. Degree in electrical engineering in 2008 from Shanghai Jiao Tong University, Shanghai, P.R. China. He is currently working toward the Ph.D. degree with the Department of Energy Technology, Aalborg University, Aalborg, Denmark.

His current research interests include wind power generation, control of permanent magnet synchronous generator, and offshore wind farm-power systems dynamics.

Zhe Chen (M'95, SM'98) received the B.Eng. and M.Sc. degrees from Northeast China Institute of Electric Power Engineering, Jilin City, China, and the Ph.D. degree from the University of Durham, Durham, U.K.

He was a Lecturer and then Senior Lecturer with De Montfort University, Leicester, U.K. Since 2002, he has been a Research Professor and now a Professor with the Institute of Energy Technology, Aalborg University, Aalborg, Denmark, where he is the coordinator of the Wind Power System Research program at the Institute of Energy Technology. His research areas are power systems, power electronics, and electric machines, with specific interest in wind energy and modern power systems. He has more than 200 publications in his technical field.

Dr. Chen is an Associate Editor (Renewable Energy) of the IEEE TRANSACTIONS ON POWER ELECTRONICS, Guest Editor of the IEEE TRANSACTIONS ON POWER ELECTRONICS (Special Issue on Power Electronics for Wind Energy Conversion). He is a Member of the Institution of Engineering and Technology (London, U.K.) and a Chartered Engineer in the U.K.